engineering proceedings

MDPI

Proceeding Paper

Functionalized 2D Germanene and Its Derivatives for Electrochemical Detection of Gut-Derived Metabolites in Human Serum †

Rachel Rui Xia Lim [1], Zdeněk Sofer [2] and Alessandra Bonanni [1,3,*]

[1] Division of Chemistry & Biological Chemistry, School of Chemistry, Chemical Engineering and Biotechnology, Nanyang Technological University, Singapore 637371, Singapore; S190110@e.ntu.edu.sg
[2] Department of Inorganic Chemistry, University of Chemistry and Technology Prague, Technicka' 5, 166 28 Prague, Czech Republic; zdenek.sofer@vscht.cz
[3] Department of Chemistry, University of Pavia, Via Taramelli 12, 27100 Pavia, Italy
* Correspondence: a.bonanni@ntu.edu.sg
† Presented at the 2nd International Electronic Conference on Chemical Sensors and Analytical Chemistry, 16–30 September 2023; Available online: https://csac2023.sciforum.net/.

Abstract: In this work, germanene and its derivatives (Ge-H, Ge-CH_3, Ge-C_3-CN) were explored as electrochemical impedimetric platforms to develop a competitive immunoassay for the direct detection of gut-derived metabolites, kynurenic acid (KA) and quinolinic acid (QA). The competition occurs between the free KA/QA standards and BSA-conjugated antigens for a fixed amount of primary antibody binding sites. This affects the electron transfer rate of the $[Fe(CN)_6]^{3-/4-}$ redox couple and changes the charge transfer resistance (R_{ct}) on the electrode surface. The impedimetric signal measured due to the change in R_{ct} is then correlated to the KA and QA concentration.

Keywords: 2D layered nanomaterials; biosensor; gut-derived metabolites; electrochemistry; electrochemical sensor; germanene; competitive immunosensor; impedance; kynurenic acid; quinolinic acid

check for updates

Citation: Lim, R.R.X.; Sofer, Z.; Bonanni, A. Functionalized 2D Germanene and Its Derivatives for Electrochemical Detection of Gut-Derived Metabolites in Human Serum. *Eng. Proc.* **2023**, *48*, 45. https://doi.org/10.3390/CSAC2023-14903

Academic Editor: Nicole Jaffrezic-Renault

Published: 26 September 2023

Copyright: © 2023 by the authors. Licensee MDPI, Basel, Switzerland. This article is an open access article distributed under the terms and conditions of the Creative Commons Attribution (CC BY) license (https://creativecommons.org/licenses/by/4.0/).

1. Introduction

Recently, abnormal levels of some gut-derived metabolites, kynurenic acid (KA) and quinolinic acid (QA) were found to be associated with neurodegenerative disorders like dementia, Alzheimer's and Parkinson's diseases [1,2]. These neurological disorders have affected more than 1 billion people worldwide and resulted in close to 7 million deaths yearly [3]. Chromatographic techniques and enzyme-linked immunosorbent assays are mostly reported in the literature to determine KA and QA [4,5]. Nevertheless, these approaches are still expensive, time-consuming, involve bulky equipment and technical expertise and they may suffer from poor sensitivity and stability [2,6,7]. Therefore, it is clinically significant to develop economical, portable, rapid and sensitive analytical methods to detect KA and QA as potential disease biomarkers for early screening and diagnosis.

Lately, among the 2D nanomaterials under Group 14, germanene derivatives with covalently terminated groups have received particular attention within the scientific community due to their increased chemical reactivity, attractive electronic and optical properties as a result of their surface functionalization [8–11]. Consisting of a hexagonal honeycomb buckled structure with sp^2/sp^3-hybridized groups [8,9,11], existing studies have demonstrated the bioconjugation and biorecognition abilities of germanene-based nanomaterials with oligonucleotides and aptamers [9,10]. Thus, in this work, we would like to explore different nanosized germanene and its derivatives as competitive electrochemical immunosensors for the direct detection of gut-derived metabolites, KA and QA as biomarkers, using disposable screen-printed carbon electrodes for the impedimetric detection. The change in charge transfer resistance (R_{ct}) of the modified electrode surface will be correlated to the

presence and absence of the analyte. So far, germanene-based nanomaterials have not been employed for such biosensing applications. Hence, this study also aims to shed light on the novel bioconjugation abilities of germanene-based nanomaterials with antigens and antibodies, as well as to highlight a promising application in the detection of gut-derived metabolites as disease biomarkers.

2. Materials and Methods

Using 0.5 g of the precursor compound $CaGe_2$, Ge-H was obtained through topochemical deintercalation of calcium with 100 mL of 35% hydrochloric acid at −30 °C. The resulting product was isolated via filtration at the end of 10 days and purified with water (5 × 200 mL) and MeOH (2 × 100 mL). Both Ge-CH_3 and Ge-C_3-CN were synthesized through the exfoliation of 0.5 g of the precursor compound $CaGe_2$ via a two-phase water-alkyl halide system for 10 days. Ge-CH_3 utilized a water/methyl iodide (5 mL) system while Ge-C_3-CN employed a water/4-bromobutanenitrile (5 mL) system. Both systems were kept in the dark under inert argon conditions for 7 days. Finally, the respective products were filtered and purified with acetone (1 × 100 mL), 1 M HCl (2 × 100 mL), water (5 × 200 mL) and MeOH (2 × 100 mL).

First, 37% hydrochloric acid, human serum (sterile-filtered from human male AB plasma, USA), kynurenic acid (KA), potassium hexacyanoferrate(II) trihydrate ($K_4[Fe(CN_6)]\cdot 3H_2O$), potassium hexacyanoferrate(III) [$K_3Fe(CN)_6$], sodium chloride (NaCl), sodium hydroxide pellets, sodium phosphate dibasic dihydrate ($Na_2HPO_4\cdot 2H_2O$) and TWEEN® 20 were bought from Sigma-Aldrich (Singapore). Quinolinic acid (QA) was obtained from Cayman Chemical (Ann Arbor, MI, USA). Antigen–antibody pairs purchased from MyBioSource (San Diego, California, USA) consisted of bovine serum albumin (BSA)-conjugated kynurenic acid (BSA-KA), polyclonal rabbit anti-general kynurenic acid primary antibody (AntiKA), BSA-conjugated quinolinic acid (BSA-QA), polyclonal rabbit anti-general quinolinic acid primary antibody (AntiQA) and none-linked caprine anti-rabbit immunoglobulin G polyclonal secondary antibody (AntiIgG). Milli-Q ion exchange column (Merck KGaA, Darmstadt, Germany) supplied ultrapure water (resistivity value of 18.2 MΩ cm at 25 °C) that was used in all experiments. Disposable screen-printed carbon electrodes were purchased from BioDevice Technology (Ishikawa, Japan).

Electrochemical impedance spectroscopy (EIS) was conducted on a μAutolab type III instrument with a frequency response analyzer (FRA2) module (Eco Chemie, Utrecht, The Netherlands). A sample volume of 20 μL was analyzed on a screen-printed electrode that consisted of a working carbon electrode, Ag/AgCl reference electrode and counter electrode at room temperature. EIS measurements were performed at a frequency range of 100 kHz to 100 mHz and a modulation amplitude of 10 mV to obtain the Nyquist plot where the data were fitted with the [$R_s(R_pC)$] equivalent circuit using NOVA 1.10 software. A constant phase element (C) was adopted due to the non-ideal behavior of the interface used. R_s (Ω) simulates the resistance of the solution while R_p (Ω) simulates the polarization resistance, which is referred to the R_{ct}. 10 mM $[Fe(CN)_6]^{3-/4-}$ in phosphate-buffered solution, PBS (5 mM $K_4[Fe(CN_6)]\cdot 3H_2O$, 5 mM [$K_3Fe(CN)_6$], 0.1 M NaCl, 0.01 M $Na_2HPO_4\cdot 2H_2O$, pH = 7.4) was used as the electrolyte. All three germanene-based nanomaterials were characterized with Fourier Transform Infrared Spectroscopy (FTIR) Shimadzu (Kyoto, Japan). Next, 300 mg of KBr powder and 1 mg of germanene material were finely ground and mixed in a mortar and pestle and transferred to a hand press to obtain the KBr pellet for analysis. Measurements of 50 scans were recorded for a wavelength range of 400 cm^{-1} to 4000 cm^{-1} and at a resolution of 4 cm^{-1}. Images on the size and morphology of the germanene-based nanomaterials were captured using the transmission electron microscopy (TEM) JEOL JEM 1400 (Tokyo, Japan) with an accelerating voltage of 100 kV and Gatan Rio9 camera in combination with the Gatan DigitalMicrograph 1.18.2 software (Pleasanton, CA, USA). Then, 3 μL of 0.5 mg/mL germanene material was drop-casted on 200-mesh lacey copper grid and dried at room temperature.

The experimental protocol was adapted from our previous work [12] with the following modifications. After 1 mg/mL germanene-based nanomaterial has been physically adsorbed onto the screen-printed carbon electrode, 3 µL of BSA-conjugated antigen (BSA-KA: 20 µg/mL; BSA-QA: 30 µg/mL) was drop-casted onto the electrode surface and dried under the heat lamp for 30 min. Thereafter, a 5 min washing step of 0.01 M PBS (pH = 7.4) was carried out at room temperature to wash off any unbound antigen in excess. Next, the material–antigen modified electrode was incubated at 37 °C in a mixture of equal volumes of primary antibody (AntiKA: 20 µg/mL; AntiQA: 30 µg/mL) and free KA/QA standards (final volume = 100 µL). After an hour of incubation, two 5 min washing steps of 0.01 M PBS + 0.05% Tween 20 (pH = 7.4) and 0.01 M PBS (pH = 7.4) were each performed at 37 °C to reduce non-specific antibody binding and rinse off any unbound primary antibodies in excess. Finally, the material–antigen–primary antibody modified electrode was incubated at 37 °C in AntiIgG secondary antibody solution (20 µg/mL for KA detection; 15 µg/mL for QA detection). Likewise, at the end of one hour incubation, two 5 min washing steps of 0.01 M PBS + 0.05% Tween 20 (pH = 7.4) and 0.01 M PBS (pH = 7.4) were each performed at 37 °C to minimize non-specific antibody binding and remove any unbound AntiIgG in excess. R_{ct} were measured after each immobilization step for comparison: (a) material, (b) antigen, (c) primary antibody, (d) secondary antibody. All incubation and washing steps were carried out at 300 rpm in the TS-100 Biosan thermoshaker.

3. Results and Discussion

3.1. Characterization of Germanene-Based Nanomaterials

3.1.1. FTIR

With reference to Figure 1, Ge-H exhibited Ge-H wagging vibrations at 559 cm^{-1}, 498 cm^{-1}, 470 cm^{-1} and strong bending GeH_2 group vibrations at around 866 cm^{-1} [9–11,13]. Ge-CH_3 displayed bending C-H vibration at 1402 cm^{-1}, C-H vibrations of methyl group at 766 cm^{-1} and Ge-C stretching band at 550 cm^{-1}, which confirms on the successful covalent attachment of the methyl groups onto the germanane sheet [9–11,14]. Similarly, Ge-C_3-CN also showed many C-H bending and rocking vibrations in the wavelength range of 1404–752 cm^{-1} [9,14]. The presence of the weak CN peak at 2297 cm^{-1}, Ge-C stretching vibration at 588 cm^{-1} and Ge-H vibrations at 500 cm^{-1}, 492 cm^{-1} indicated the successful covalent functionalization of the characteristic groups in Ge-C_3-CN [9,14,15]. The Ge-C_3-CN spectrum had a trace amount of water present at around 3426 cm^{-1} (O-H stretching vibration), which could be due to some moisture inevitably being absorbed during sample preparation and analysis. Overall, these FTIR results serve as an affirmation on the successful synthesis of the various functionalized germanene-based nanomaterials used in our study.

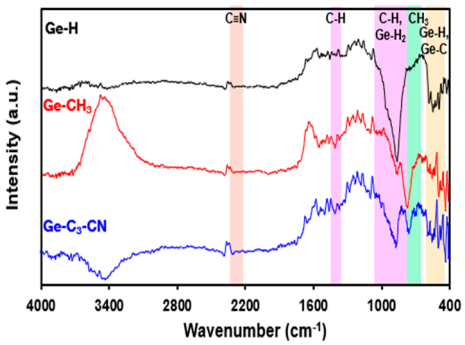

Figure 1. FTIR spectra of Ge-H, Ge-CH_3 and Ge-C_3-CN (using KBr pellet as blank).

3.1.2. TEM

Figure 2 depicted smooth sheet-like pieces with a few stacked layers for Ge-H, Ge-CH_3, Ge-C_3-CN, which were consistent with the published literature on germanene morphologies [8–10]. From Figure 2, the lateral size of Ge-H was approximately 217 nm while

the lateral sizes of Ge-CH_3 and Ge-C_3-CN were 867 nm and 1133 nm, respectively. It is worth noting the differences in material size as it could potentially influence the material's bioconjugation ability with biomolecules and the detection sensitivity towards the analyte.

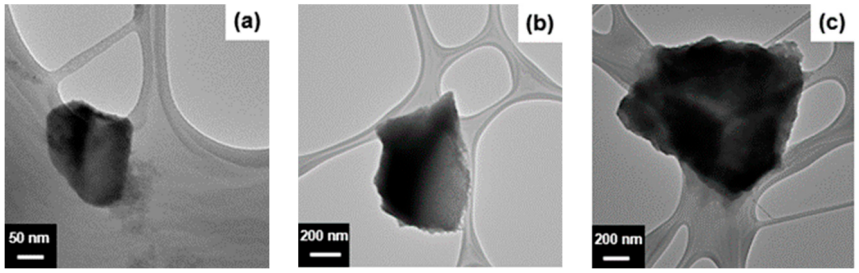

Figure 2. TEM images of germanene-based nanomaterial on lacey carbon supported copper grids (**a**) Ge-H; (**b**) Ge-CH_3; (**c**) Ge-C_3-CN.

3.2. Performance of Germanene-Based Nanomaterials

To select the best performing germanene-based nanomaterial to proceed with the calibration study, the change in R_{ct} signals of Ge-H, Ge-CH_3 and Ge-C_3-CN were measured and compared at the last step, after the addition of the secondary antibody, AntiIgG.

Among the three germanene-based nanomaterials, it seems like Ge-H is the ideal material to be used in this study. Even though Ge-H was the smallest in size and functionalized with the smallest hydrogenated group as shown in Figures 1 and 2, it was able to produce the highest signal in terms of R_{ct} difference with respect to the material (Figure 3b). This suggests that Ge-H was the most sensitive towards the addition of antigens and antibodies since it gave the largest change in R_{ct} upon the interaction with the secondary antibody, AntiIgG at the final step. The size and type of functional groups could play a part in this phenomenon. As mentioned previously in Figures 1 and 2, Ge-CH_3 and Ge-C_3-CN were much larger in size and contained the methyl and cyanopropyl substituents, respectively. This might have resulted in Ge-CH_3 and Ge-C_3-CN being more sterically hindered than Ge-H, which could slow down the heterogenous electron transfer of the materials and affect their sensing performance.

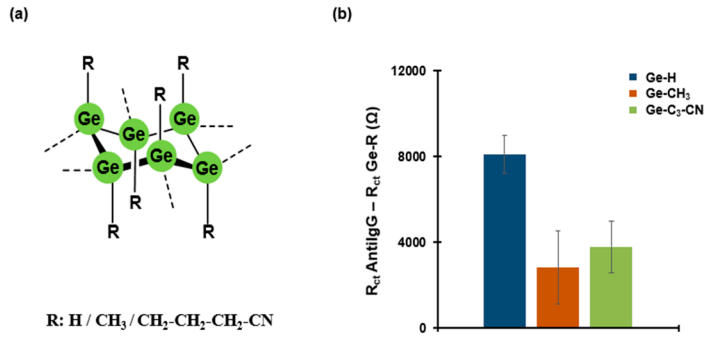

Figure 3. (**a**) General structure of germanene and its derivatives; (**b**) R_{ct} variations of Ge-H, Ge-CH_3 and Ge-C_3-CN. Conditions: 1 mg/mL germanene-based nanomaterial, 0.01 mg/mL BSA-KA, 50 µg/mL AntiKA and 50 µg/mL AntiIgG, 10 mM $[Fe(CN)_6]^{3-/4-}$ in PBS buffer (pH 7.4).

3.3. Calibration Study

The detection principle of the proposed electrochemical immunosensor is primarily based on the competition between the free antigens in the solution and the BSA-conjugated antigens immobilized onto the modified electrode surface. As the concentration of the free standards in the mixture increases, there will be more interaction between the free standards and primary antibodies. Consequently, fewer primary antibodies will be left on the electrode surface to interact with the secondary antibodies that were added subsequently. Since the electron transfer process of the $[Fe(CN)_6]^{3-/4-}$ redox couple on the

screen-printed electrode surface is now less hindered, a lower R_{ct} will be measured. Thus, this accounts for the downward trend observed for both KA and QA (Figure 4).

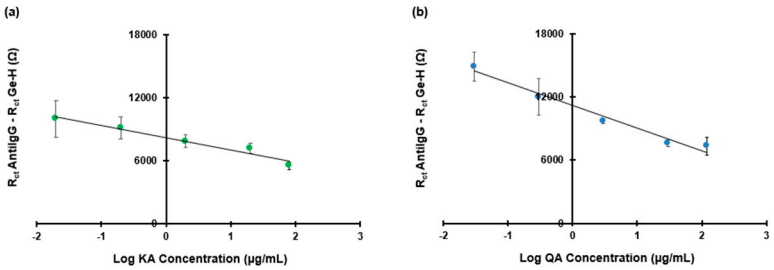

Figure 4. (R_{ct} AntiIgG—R_{ct} Ge-H) values against log concentration of free standards: (**a**) 0.02–80 µg/mL KA; (**b**) 0.03–120 µg/mL QA. Conditions: 1 mg/mL Ge-H, 10 mM $[Fe(CN)_6]^{3-/4-}$ in PBS buffer (pH 7.4), (**a**) 20 µg/mL BSA-KA, 20 µg/mL of AntiKA, 20 µg/mL of AntiIgG; (**b**) 30 µg/mL BSA-QA, 30 µg/mL of AntiQA, 15 µg/mL of AntiIgG.

Based on the high slope values (1160–2151 Ω/(µg/mL)) obtained from the calibration plots, the Ge-H immunosensor was sensitive in the detection of KA and QA. Additionally, it was able to achieve strong linearity (0.9597–0.9750) and low limits of detection of 0.08–27 ng/mL (0.42–161 nM) in the detection of KA and QA. Furthermore, the feasibility of the proposed immunosensor was successfully tested on real serum sample from a healthy individual, where the KA and QA amounts detected were 9.14–798.45 ng/mL (48.3 nM–4.78 µM) at relative standard deviation values of 4.4–11.3%.

4. Conclusions

In this preliminary study, we have successfully demonstrated the bioconjugation abilities of germanene-based nanomaterials with antigens and antibodies as well as a new application in the detection of gut-derived metabolites as disease biomarkers. Among the three materials, Ge-H was the best-performing material due to its smallest size with the smallest hydrogen group substituent, as shown in FTIR and TEM when compared with Ge-CH_3 and Ge-C_3-CN. This helps Ge-H to be less sterically hindered than Ge-CH_3 and Ge-C_3-CN during the different bioconjugation steps and speed up the heterogenous electron transfer rate on the material surface. Coupled with the low-cost, easily miniaturized and portable screen-printed carbon electrode, our proposed Ge-H electrochemical immunosensor is fast, sensitive and stable for widespread accessibility, especially in low-income and resource-limited places, making them as promising point-of-care devices in clinical analysis.

Author Contributions: Conceptualization, A.B.; methodology, R.R.X.L.; validation, R.R.X.L.; investigation, R.R.X.L.; synthesis and provision of study materials, Z.S.; writing—original draft preparation, R.R.X.L.; writing—review and editing, A.B.; supervision, A.B.; funding acquisition, A.B. All authors have read and agreed to the published version of the manuscript.

Funding: The authors gratefully acknowledge Ministry of Education (MOE) Singapore, AcRF Tier 1 grant (Reference No: RG88/20) and Czech Science Foundation (GACR No. 19-26910X) for the financial support.

Institutional Review Board Statement: Not applicable.

Informed Consent Statement: Not applicable.

Data Availability Statement: Data sharing not applicable.

Conflicts of Interest: The authors declare no conflict of interest. The funders had no role in the design of the study; in the collection, analyses, or interpretation of data; in the writing of the manuscript; or in the decision to publish the results.

References

1. Karle, A.; Twum, K.; Sabbagh, N.; Haddad, A.; Taimoory, S.M.; Szczesniak, M.M.; Trivedi, E.; Trant, J.F.; Beyeh, N.K. Naphthalene-functionalized resorcinarene as selective, fluorescent self-quenching sensor for kynurenic acid. *Analyst* **2022**, *147*, 2264–2271. [CrossRef] [PubMed]
2. Zhang, B.D.; Liu, B.; Yin, Y.X.; Xu, L. Samarium-Based Turn-Off Fluorescence Sensor for Sensitive and Selective Detection of Quinolinic Acid in Human Urine and Serum. *Inorg. Chem.* **2023**, *62*, 1007–1017. [CrossRef] [PubMed]
3. Neurological Disorders Affect Millions Globally: WHO Report. Available online: https://www.who.int/news/item/27-02-2007-neurological-disorders-affect-millions-globally-who-report (accessed on 21 April 2023).
4. Fukushima, T.; Umino, M.; Sakamoto, T.; Onozato, M. A review of chromatographic methods for bioactive tryptophan metabolites, kynurenine, kynurenic acid, quinolinic acid, and others, in biological fluids. *Biomed. Chromatogr.* **2022**, *36*, e5308. [CrossRef] [PubMed]
5. Sadok, I.; Gamian, A.; Staniszewska, M.M. Chromatographic analysis of tryptophan metabolites. *J. Sep. Sci.* **2017**, *40*, 3020–3045. [CrossRef] [PubMed]
6. Singh, R.; Kashayap, S.; Singh, V.; Kayastha, A.M.; Mishra, H.; Saxena, P.S.; Srivastava, A.; Singh, R.K. QPRTase modified N-doped carbon quantum dots: A fluorescent bioprobe for selective detection of neurotoxin quinolinic acid in human serum. *Biosens. Bioelectron.* **2018**, *101*, 103–109. [CrossRef] [PubMed]
7. Oh, J.S.; Seo, H.S.; Kim, K.H.; Pyo, H.; Chung, B.C.; Lee, J. Urinary profiling of tryptophan and its related metabolites in patients with metabolic syndrome by liquid chromatography-electrospray ionization/mass spectrometry. *Anal. Bioanal. Chem.* **2017**, *409*, 5501–5512. [CrossRef] [PubMed]
8. Liu, N.; Bo, G.; Liu, Y.; Xu, X.; Du, Y.; Dou, S.X. Recent Progress on Germanene and Functionalized Germanene: Preparation, Characterizations, Applications, and Challenges. *Small* **2019**, *15*, e1805147. [CrossRef] [PubMed]
9. Song, Z.; Ang, W.L.; Sturala, J.; Mazanek, V.; Marvan, P.; Sofer, Z.; Ambrosi, A.; Ding, C.; Luo, X.; Bonanni, A. Functionalized Germanene-Based Nanomaterials for the Detection of Single Nucleotide Polymorphism. *ACS Appl. Nano Mater.* **2021**, *4*, 5164–5175. [CrossRef]
10. Ang, W.L.; Sturala, J.; Antonatos, N.; Sofer, Z.; Bonanni, A. Effect of surface chemistry on bio-conjugation and bio-recognition abilities of 2D germanene materials. *Nanoscale* **2021**, *13*, 1893–1903. [CrossRef] [PubMed]
11. Rosli, N.F.; Rohaizad, N.; Sturala, J.; Fisher, A.C.; Webster, R.D.; Pumera, M. Siloxene, Germanane, and Methylgermanane: Functionalized 2D Materials of Group 14 for Electrochemical Applications. *Adv. Funct. Mater.* **2020**, *30*, 1910186. [CrossRef]
12. Cheng, Z.X.; Ang, W.L.; Bonanni, A. Electroactive Nanocarbon Can Simultaneously Work as Platform and Signal Generator for Label-Free Immunosensing. *ChemElectroChem* **2019**, *6*, 3615–3620. [CrossRef]
13. Kovalska, E.; Antonatos, N.; Luxa, J.; Sofer, Z. Edge-Hydrogenated Germanene by Electrochemical Decalcification-Exfoliation of CaGe(2): Germanene-Enabled Vapor Sensor. *ACS Nano* **2021**, *15*, 16709–16718. [CrossRef] [PubMed]
14. Hartman, T.; Sturala, J.; Luxa, J.; Sofer, Z. Chemistry of Germanene: Surface Modification of Germanane Using Alkyl Halides. *ACS Nano* **2020**, *14*, 7319–7327. [CrossRef] [PubMed]
15. Jiang, S.; Krymowski, K.; Asel, T.; Arguilla, M.Q.; Cultrara, N.D.; Yanchenko, E.; Yang, X.; Brillson, L.J.; Windl, W.; Goldberger, J.E. Tailoring the Electronic Structure of Covalently Functionalized Germanane via the Interplay of Ligand Strain and Electronegativity. *Chem. Mater.* **2016**, *28*, 8071–8077. [CrossRef]

Disclaimer/Publisher's Note: The statements, opinions and data contained in all publications are solely those of the individual author(s) and contributor(s) and not of MDPI and/or the editor(s). MDPI and/or the editor(s) disclaim responsibility for any injury to people or property resulting from any ideas, methods, instructions or products referred to in the content.